Bidimensional Analysis of a Thermoelectric Module using Finite Element Techniques

*Antonio Arenas, Jorge Vázquez, Rafael Palacios
Universidad Pontificia Comillas
Escuela Técnica Superior de Ingeniería
*Departamento de Fluidos y Calor, Instituto de Investigación Tecnológica
Alberto Aguilera, 23
28015 Madrid (Spain)
e_mail: arenas@dfc.icai.upco.es

Abstract

In this paper an analysis is performed on a thermoelectric module using finite element techniques taking into account the following two hypothesis: thermal and electrical flows are present in two dimensions.

The commercial software tool named ANSYS has been used in order to develop this analysis. This software includes the possibility to analyse jointly the *Fourier* and *Joule* effects, but not the *Peltier* effect. Additional software has been developed in order to include the *Peltier* effect. The consideration of the three effects at the same time will allow for a better simulation and analysis of the performance of a thermoelectric module.

The ANSYS model developed very closely represents the real configuration of a thermoelectric module. It takes into account the thermoelements, and their electrical bridges and junctions. All the properties of the materials have been considered constant.

Several simulations have been performed using the proposed model. In all cases, the model has become a powerful and flexible tool of analysis able to present detailed numerical and graphical results. Furthermore, the possibility to use this model in more complex structures is a very attractive feature now available. The comparison between the results of this model and the performance of an elemental thermoelement allows the observation of the influence of every component in a thermoelectric module. The model and the main tests performed will be presented in this paper.

Introduction

Numeric techniques are necessary when a detailed analysis of a thermoelectric cell is required. In this work a finite element model was developed using tools probed enough to guarantee its reliability. Only a specific subroutine was designed and programmed in APDL (ANSYS Parametric Design Language).

The study of the behaviour of a thermoelectric cell is basically a problem of simultaneous thermal and electrical flows in a regular geometry. ANSYS, a commercial program of finite element method, solves this type of problems with high accuracy as stated a lot of validated tests.

All the models in this work were studied in two dimensions. It is a good approximation because the electrical and thermal flows are distributed in two dimensions in the thermoelements, electrical bridges, and soldering paste. There will be only thermal flux in 3D in the heat exchange plates. So, the results of this study are completely valid for the internal elements of the cell.

Structure of the program

The program allows introducing parametric models and making simulations with a great deal of loads and boundary conditions.

The program has a main subroutine that controls two auxiliary subroutines: a data subroutine where all the values of the variables are introduced; and the Peltier subroutine, where Peltier effect is applied.

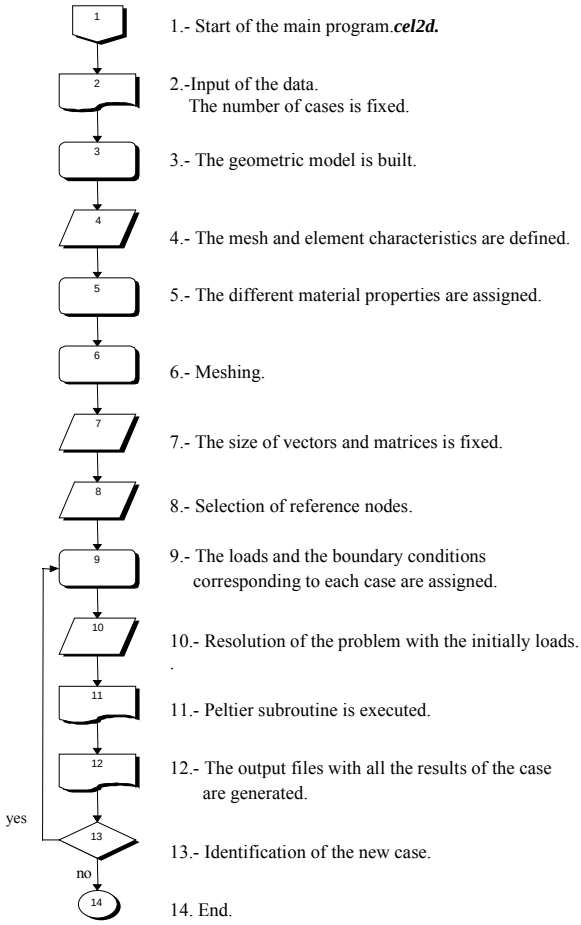

Figure 1. Main subroutine flow chart.

Main subroutine

The flow chart of the main subroutine is shown in Fig. 1.

ANSYS provides two types of elements (PLANE 67 and SOLID 69) for problems of thermal and electrical flows, but it does not have any element that takes into account Peltier, Fourier and Joule effects simultaneously.

The mesh has the same shape in the thermoelectric cell but it does not have the same size in all the components. As the

cell has a layered structure, it was easy to get the coincidence of the nodes located in the contiguous surfaces. In other words, all the elements of the mesh have the same base dimension and they only differ in its height.

Data subroutine

All the data regarding with the cell (dimensions, material properties, loads and boundary conditions), and some variables to control the program and the presentation of the results are included in this subroutine.

Peltier subroutine

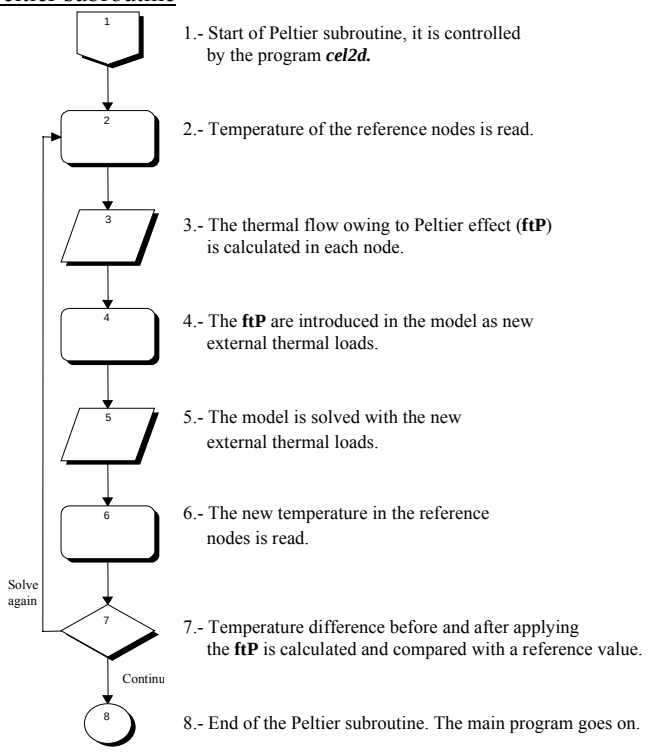

Figure 2. Flow chart of Peltier subroutine.

A specific subroutine was programmed in order to apply the Peltier effect in the model. The flow chart of this subroutine is shown in Fig.2.

The temperature and electrical current density in all the nodes of the mesh are stored. With these data the thermal power by Peltier effect is calculated and applied as a new external load in each of the nodes in the corresponding direction.

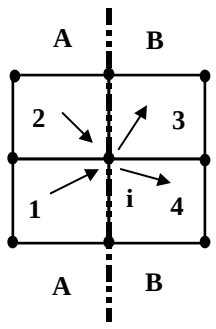

Figure 3. Scheme of the mesh.

Peltier effect is produced in the separation surfaces between two different materials when electrical current goes across it. The algorithm is able to discriminate the nodes that are in the separation surfaces and then calculates the current that crosses it. The program also takes into account the discontinuity of the materials in the ends of the model (inlet and outlet of the electrical current)

A piece of the mesh is shown in Fig. 3, it brings together the four elements around a generic node, being **j=1,2,3,4** the elements which has the node **i** in common.

A node can belong to several elements (an element is each of the small quadrilaterals in which the model is meshed). Every component of the thermoelectric cell is divided into elements and a material is assigned to every element in the model. Firstly, the following product is calculated for each node as a part of an element:

$$\dot{Q}_{p_{ij}} = I_{ij}\sigma_{ij}T_i \tag{1}$$

where:

$\dot{Q}_{p_{ij}}$: *Peltier* heat in node **i** associated with the element **j**

I_{ij} : Intensity in node **i** associated with the element **j**.

T_i : Temperature at node **i**.

σ_{ij} : *Seebeck* coefficient in node **i** associated with element **j**

The sum of all the products, $\dot{Q}_{p_{ij}}$,is the net heat generated by Peltier effect in the influence area of node *i* (the same influence area that for the intensities I_{ij} assigned to each node):

$$\dot{Q}_{p_i} = \sum_j T_i\sigma_{ij}I_{ij} = T_i\sum_j \sigma_{ij}I_{ij} \tag{2}$$

$$\sum_j I_{ij} = 0 \tag{3}$$

The sign of $\dot{Q}_{p_{ij}}$ is given by the electrical current. Then, all the $\dot{Q}_{p_{ij}}$ are applied as new external loads and the problem is solved again as a thermal and electrical one. A new temperature and current density distribution is obtained. This process will be repeated until the distributions between two consecutive iterations will be practically invariable.

The electrical current can be written as:

$$I_{ij} = I_{i(j,j+1)} + I_{i(j,j-1)} \tag{4}$$

Where the subscript $i(j, j\pm1)$ means the line of separation between the adjacent elements j and $j\pm1$ around the node i. Then:

$$I_{ij}\sigma_{ij} = \left(I_{i(j,j+1)} + I_{i(j,j-1)}\right)\sigma_{ij} = I_{i(j,j+1)}\sigma_{ij} + I_{i(j,j-1)}\sigma_{ij} \tag{5}$$

Calculating the sum of all these products for all the elements that have the node i in common, the eq. (6) is obtained:

$$\dot{Q}_{p_i} = T_i\sum_j\left(I_{ij}\sigma_{ij}\right) = T_i\sum_j\left(I_{i(j,j+1)}\bullet\left(\sigma_{ij} - \sigma_{ij+1}\right)\right) \tag{6}$$

In Fig. 3, elements 1-2 and 3-4 have the same materials assigned, so $\sigma_{i1} = \sigma_{i2}$ and $\sigma_{i3} = \sigma_{i4}$. In this case, the eq. (6) will be:

$$\dot{Q}_{pi} = T_i\left(I_{i(1,4)} + I_{i(2,3)}\right)\left(\sigma_A - \sigma_B\right) \tag{7}$$

$$\dot{Q}_{pi} = T_i I_i (\sigma_A - \sigma_B) \quad (8)$$

Being $\dot{Q}_{pi} > 0$ when the heat is generated in the union.

Analysed cases

Two cases were studied:

- An elemental constant case (***2d-ec***): it uses a simplified model with isotropic materials and with constant properties. The model was also studied with analytical equations in order to verify the results obtained with the program.
- A complete constant case (***2d-cc***): a thermoelectric cell with all the elements (electrical bridges, weldings...) was studied. The material properties were considered constant with the temperature.

All simulations were done with a constant electrical current and fixing the temperature on the hot and cold faces of the thermoelectric cell. Normally, these are the reference conditions in the catalogues of the manufacturers, although some times, the heat transmission between the cell and the ambient can cause very important limitations, being critic the size of the cold and hot faces in the design and operation of the cell [2].

Elemental-constant model 2d-ec

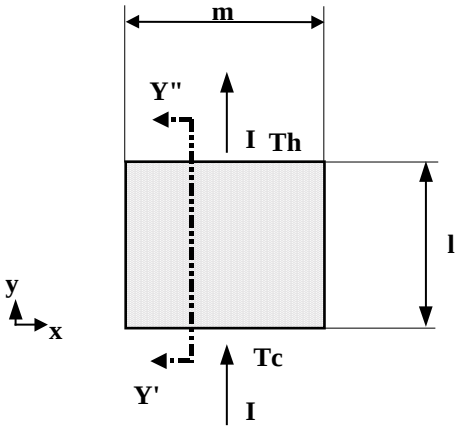

Figure 4. Scheme of the model 2d-ec.

The elemental model was only made up by the thermoelements joined by a material without thermal and electrical resistance. This model is physically infeasible but very useful in a theoretical analysis.

As shown in Fig. 4, it is possible to use only a thermoelement whose properties are the average of each of the two thermoelements (type p and n) that form the thermocouple. The dimensions were l=1.14 mm and m=1.4 mm. Materials and properties can be seen in annexe 1.

The model worked with the cold face temperature fixed at Tc=273K. Different cases were studied corresponding to temperature differences (Th-Tc) from 0ºC to 70ºC with increments of 10ºC, and electrical current varying from 1A to 7A with increments of 1A (56 cases in total).

All the results lacked of interest if they were not compared with the analytical ones obtained in [1, chapter 2], because the theoretical equations are exact in this simplified model. All the results presented in next figures are the relative differences between de magnitudes calculated by the numerical method "n" and the analytical one "a", $(X_n - X_a)/X_a$.

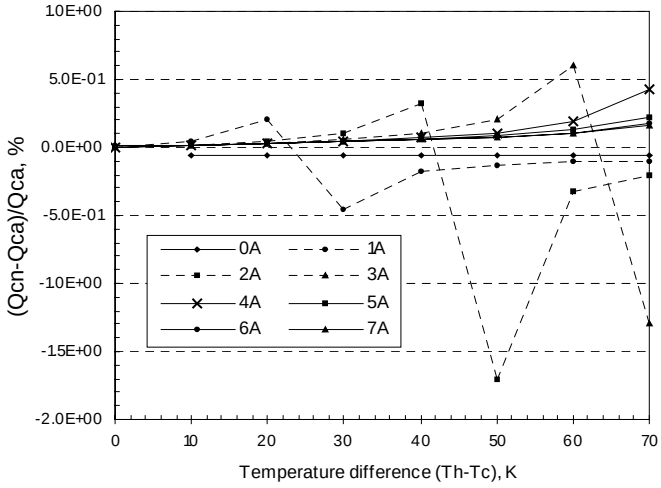

Figure 5. Relative difference in Qc.Mode A.Tc=273K (2d-ec).

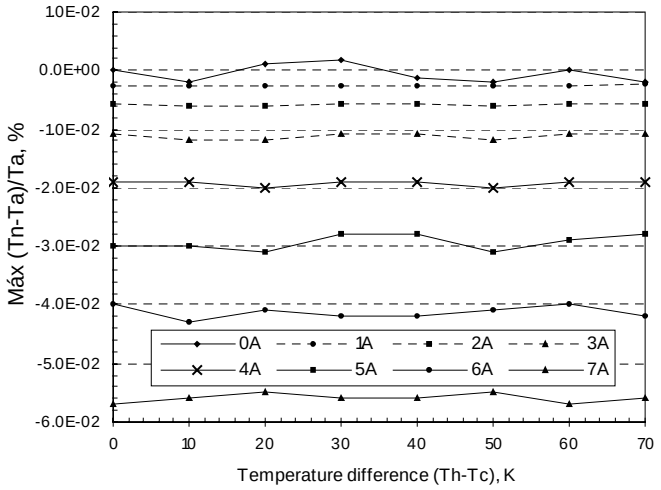

Figure 6. Maximum relative differences in the temperature distribution inside the thermoelement.

The relative differences in thermal powers are very low, being under 0.2% for $\dot{Q}_c$ and 0.02% for $\dot{Q}_h$, except in the proximities of the change of sign. In the case of the thermal power generated by Peltier effect the error is negligible, and this is the most important conclusion because it was the main objective of this analysis. The relative difference between the efficiencies is also very low, under 0.02% and it is always very similar to the difference of the thermal powers.

At last, the temperature distribution was evaluated in the cross section (Y'-Y''). As shown in Fig. 6, the maximum relative difference is less than 0.06%, being the temperature calculated by the numerical method always lower than the analytical.

Complete-constant model 2d-cc

The model simulated is shown in Fig. 7, the dimensions and materials are specified in annexe 1. In this case the model takes into account all the materials involved in a commercial thermoelectric module. The model includes:

- The weldings (elements b*x*) between the thermoelements (a*x*) and electrical conductors (c*x*)

- The dimension in z direction is 1mm. (2D).
- The material properties are considered constant.
- The size of the mesh is 0.1mm.

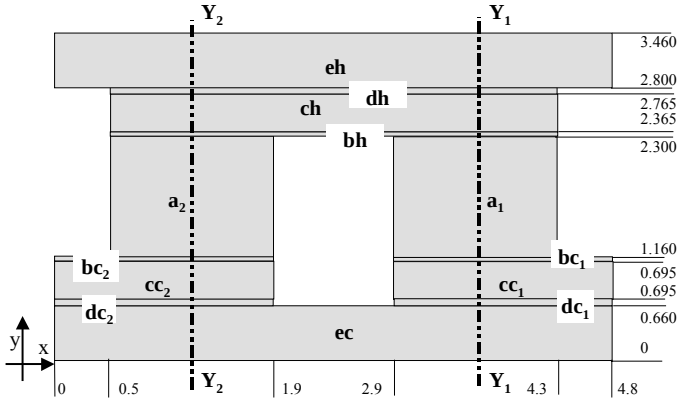

Figure 7. Scheme of the model 2d-cc, dimensions (mm).

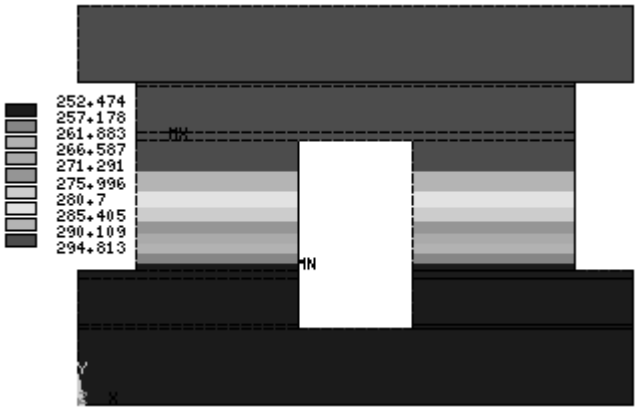

Figure 8. Temperatures, Tc=273K, $\Delta T = 40^{\circ}C$, I=4A.

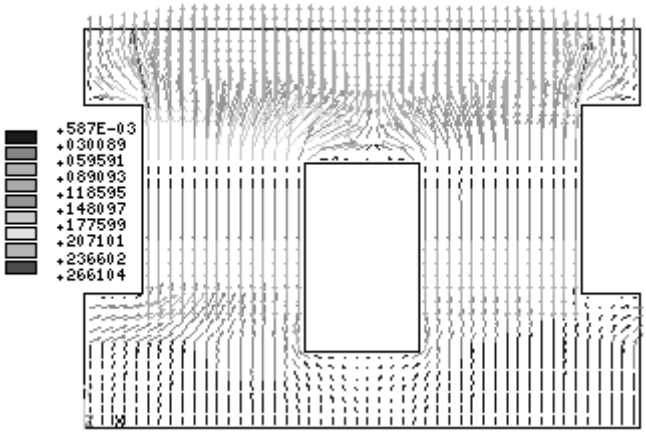

Figure 9. Heat power flow (W/m^2), Tc=273K $\Delta T = 40^{\circ}C$, I=4 A.

In this case, it is possible to reproduce the way of working of a thermoelectric cell studying a thermocouple owing to the symmetry, but the model cannot be reduced to a unique thermoelement.

Two ways of working were analysed. The first mode (Mode A) in which the cold face temperature remained constant (Tc=273K), and the second one (Mode B) in which the hot face temperature was fixed in (Th=293K). The same temperature differences and electrical currents as in the model "2d-ec" were studied. ANSYS allows to plot the temperature distribution in all nodes, and the thermal and electrical flow (Figs. 8, 9, 10).

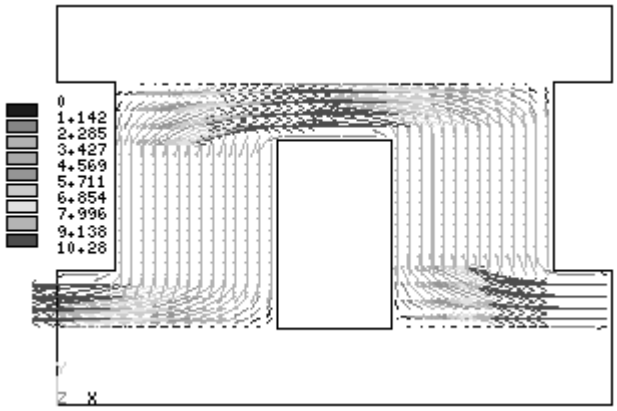

Figure 10. Electric current flow (A/m^2).
Tc=273K, $\Delta T = 40^{\circ}C$, I=4 A.

Efficiency (ε_f) (Mode A) and *COP* (Mode B).

The ε_f and *COP* associated with mode A and mode B respectively are shown in Tables 1 and 2.

I \ ΔT	0ºC	10ºC	20ºC	30ºC	40ºC	50ºC	60ºC	70ºC
0 A	-	-	-	-	-	-	-	-
1 A	6.645	3.229	0.987	-0.598	-1.778	-2.690	-3.387	-3.976
2 A	3.074	2.150	1.417	0.800	0.317	-0.090	-0.439	-0.740
3 A	1.884	1.470	1.086	0.789	0.531	0.304	0.102	-0.078
4 A	1.289	1.026	0.828	0.652	0.494	0.351	0.221	0.103
5 A	0.933	0.761	0.634	0.519	0.413	0.316	0.227	0.145
6 A	0.695	0.574	0.487	0.406	0.332	0.263	0.198	0.138
7 A	0.526	0.435	0.373	0.314	0.259	0.208	0.160	0.114

Table 1. Efficiency ε_f (%), Mode A. T_c=273K

I \ ΔT	0ºC	10ºC	20ºC	30ºC	40ºC	50ºC	60ºC	70ºC
0 A	-	-	-	-	-	-	-	-
1 A	8.169	4.437	1.987	0.255	-1.034	-2.030	-2.795	-3.440
2 A	4.335	3.265	2.417	1.709	1.149	0.676	0.272	-0.078
3 A	3.058	2.550	2.086	1.722	1.405	1.126	0.877	0.656
4 A	2.420	2.085	1.828	1.599	1.393	1.207	1.038	0.884
5 A	2.037	1.808	1.634	1.475	1.329	1.196	1.072	0.958
6 A	1.783	1.614	1.487	1.369	1.260	1.159	1.064	0.976
7 A	1.601	1.470	1.373	1.282	1.197	1.117	1.042	0.971

Table 2. Coefficient of Performance (*COP*),Mode B. T_h=293K

The values obtained with the numerical method were compared with the corresponding results of the elementary model (e), which represent the maximum values for each working condition.

As shown in Figs 11 and 12, the ε_f was reduced in a 18% compared with its maximum value. This drop is attributed to the elements in between (weldings, electrical bridges...). However, the decrease in *COP* was less significant because the reference values are higher.

The results for ε_f and *COP* obtained in the complex numerical model were in agreement with the results derived from the analytical model indicated in [1, chapter 5]. As shown in Figs. 13 and 14, the relative differences are under 6% and 1% in ε_f and *COP* respectively.

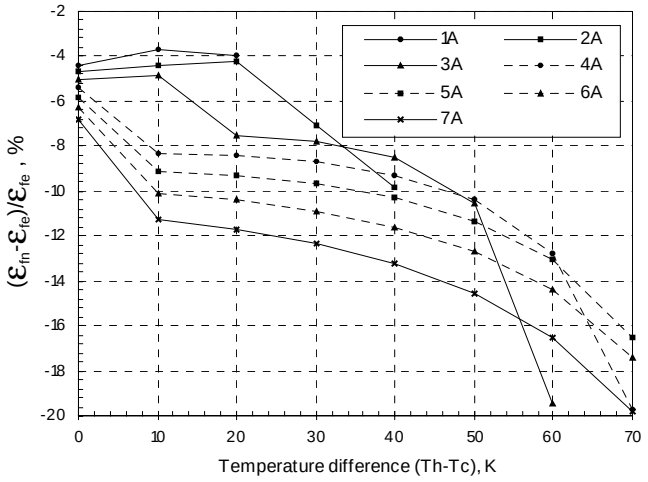

Figure 11. Relative differences in ε_f compared to the elementary model. Mode A, T_c=273K.

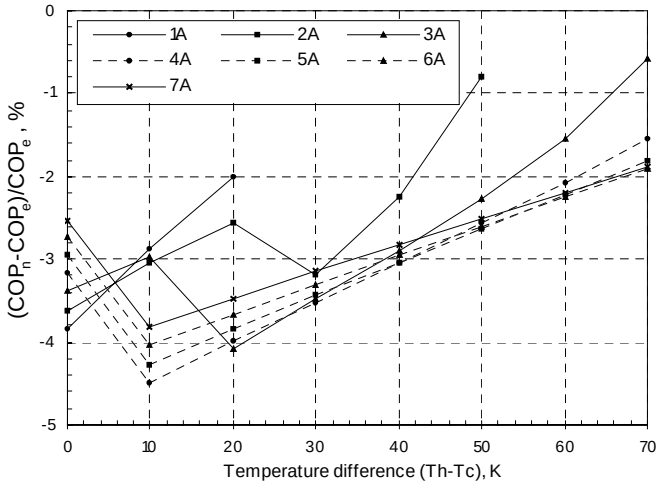

Figure 12. Relative differences in COP compared to the elementary model. Mode B, T_h=293K.

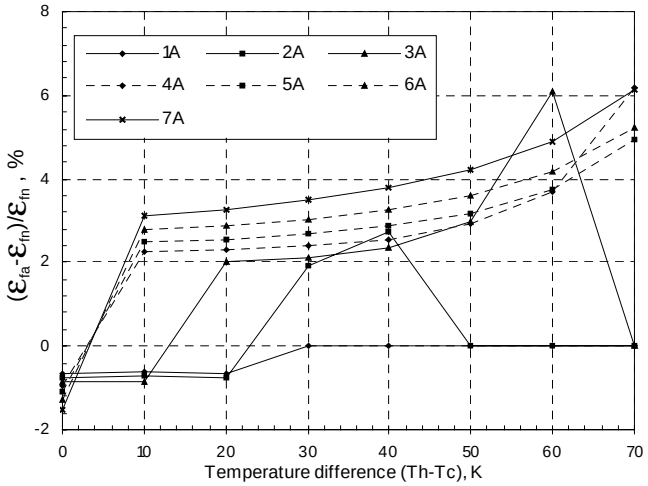

Figure 13. Relative differences in ε_f compared to the analytical model. Mode A, T_c=273K.

The point in which the cell works with maximum efficiency is considered the most relevant. So, the relative differences between the complex model and the elementary model working at this point constitutes the most important measure of the influence of the additional components that built a real thermoelectric cell. These differences fluctuated from 3% to 17% in ε_f and were lower than 4% in the case of *COP*.

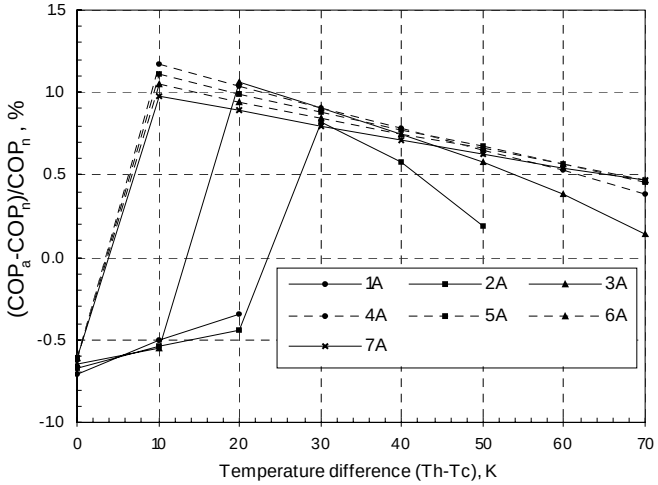

Figure 14. Relative differences in COP compared to the analytical model. Mode B, T_h=293K.

Thermal powers

The graphs of thermal powers on the cold face ($\dot{Q}_c$, mode A) and on the hot face ($\dot{Q}_h$, mode B) versus the temperature difference are shown in Figs. 15 and 16.

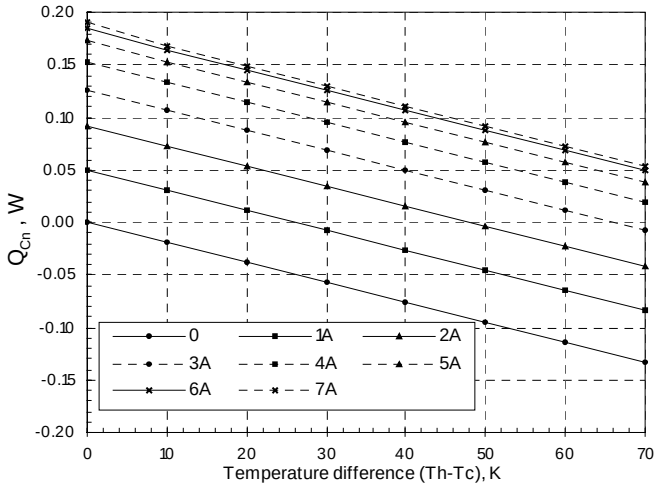

Figure 15.Thermal power at cold face. $\dot{Q}_c$. Mode A. T_c=273K.

A detailed analysis of the total thermal power density in the hot and cold face of the cell was carried out. As stated in Figs. 17 and 18, the absence of uniformity is clear in both distributions. In the hot face the maximum value is reached at x=1.3mm and it is 17.5% higher than the average, while the minimum is at x=4.8mm and it is 39.8% lower. The distribution on the cold face is less uniform, with the maximum located at x=1.1mm (34.24%) while the minimum is at x=2.5mm (-39.27%).

Despite of the geometric symmetry, there is an asymmetry in the thermal power density distributions. The reason of this asymmetry lies on the difference in the Seebeck coefficients between the thermoelements and the adjacent materials.

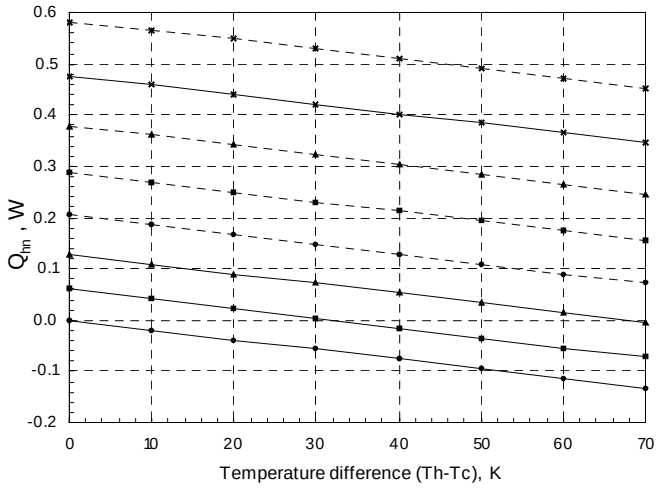

Figure 16. Thermal power at hot face, $\dot{Q}_h$. Mode B. T_h=293K.

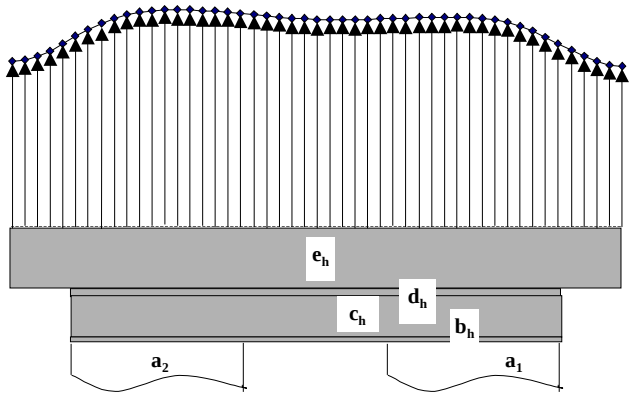

Figure 17. Total thermal power density at hot face. T_c=273K, $\Delta T = 40^{\circ}\mathrm{C}$, I=4A.

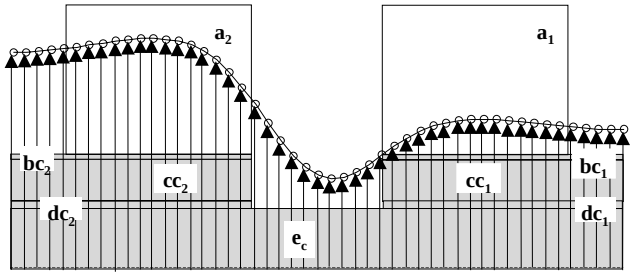

Figure 18. Total thermal power density at cold face. T_c=273K, $\Delta T = 40^{\circ}\mathrm{C}$, I=4A.

If σ_{t1}, σ_{t2}, and σ_{bh} are the Seebeck coefficients of a1, a2, and b_h (Fig. 16), the thermal power produced by Peltier effect at the hot face of each thermoelement is:

$$\dot{Q}_{Ph1} = \sum_{n\to 2,9}^{n\to 4,3} I_n T_n \left(\sigma_{bh} - \sigma_{t1}\right) \tag{9}$$

$$\dot{Q}_{Ph2} = \sum_{n\to 0,5}^{n\to 1,9} I_n T_n \left(\sigma_{t2} - \sigma_{bh}\right) \tag{10}$$

Normally $\sigma_{t1} = -\sigma_{t2}$ and then:

$$\sigma_{bh} - \sigma_{t1} = \left(\sigma_{t2} - \sigma_{bh}\right) + 2\sigma_{bh} \tag{11}$$

If it is admitted the same number of nodes (n), a uniform temperature distribution ($T_n = T$), and a uniform electrical current distribution ($I_n = I/n$), then:

$$\dot{Q}_{Ph1} - \dot{Q}_{Ph2} = 2 \cdot I \cdot T \cdot \sigma_{bh} \tag{12}$$

However, under the same conditions, the sum of $\dot{Q}_{Ph1}$ and $\dot{Q}_{Ph2}$ is the same as in a direct contact between the thermoelements without welding or other elements.

$$\dot{Q}_{Ph1} + \dot{Q}_{Ph2} = \sum_{n\to 0,5}^{n\to 1,9} I_n T_n \left(\sigma_{t1} - \sigma_{t2}\right) + \sum_{n\to 2,9}^{n\to 4,3} I_n T_n \left(\sigma_{t1} - \sigma_{t2}\right) \tag{13}$$

$$\dot{Q}_{Ph1} = \dot{Q}_{Ph2} = \frac{1}{2}\left[\sum_{n\to 0,5}^{n\to 1,9} I_n T_n \left(\sigma_{t2} - \sigma_{t1}\right) + \sum_{n\to 2,9}^{n\to 4,3} I_n T_n \left(\sigma_{t2} - \sigma_{t1}\right)\right] \tag{14}$$

$$\dot{Q}_{Ph1} = \dot{Q}_{Ph2} = \sum_{n\to 0,5}^{n\to 1,9} I_n T_n \sigma_{t2} = \sum_{n\to 2,9}^{n\to 4,3} I_n T_n \sigma_{t2} \tag{15}$$

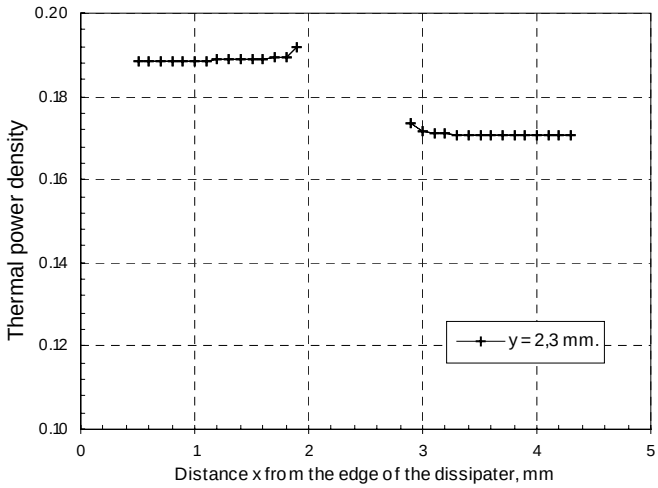

Figure 19. Thermal power density (W/mm^2) by *Peltier* effect in the hot side of the thermoelements. Tc=273K, ΔT=40ºC, I=4A.

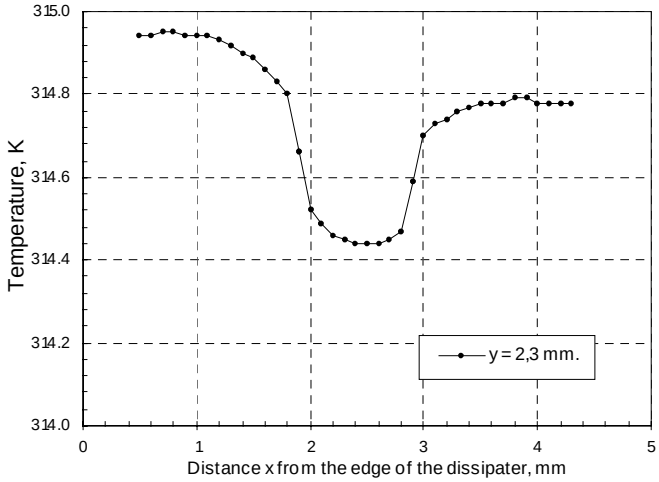

Figure 20. Temperature distribution in element **bc.**

The lack of uniformity in the thermal power density (Fig. 19) in the internal side of the thermoelements is owing to the higher electrical current density in this area and because the drop in temperature in this area (Fig. 20) is very small. This

drop of temperature is so small firstly, because the thermal conductivity of the soldering paste is very high and secondly because the high current density produces an important rise in the thermal power generated by Joule effect increasing the temperatures. This short of uniformity can be more important if the material properties are considered variable with the temperature.

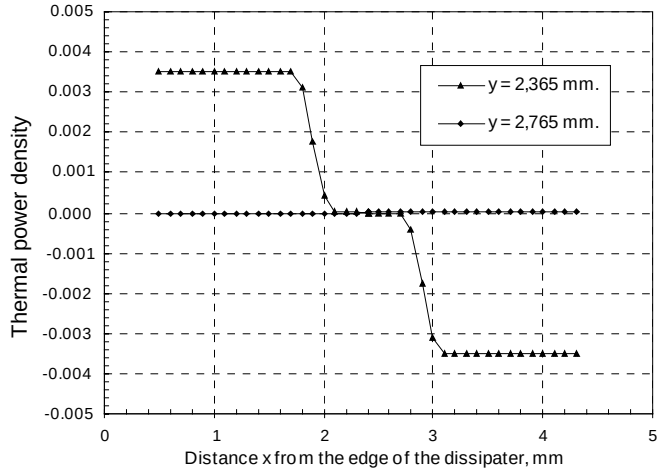

Figure 21. Thermal power density (W/mm^2) by Peltier effect in the hot side of the cell. T_c=273K, $\Delta T = 40^{\circ}\mathrm{C}$, I=4ª.

As shown in Fig. 21, the Peltier power density in the unions of the additional elements is completely symmetric in both sides of the thermoelements (a1, a2). As the electrical current crosses the elements in opposite direction, the sign of this power is different and the net contribution to the thermocouple is null.

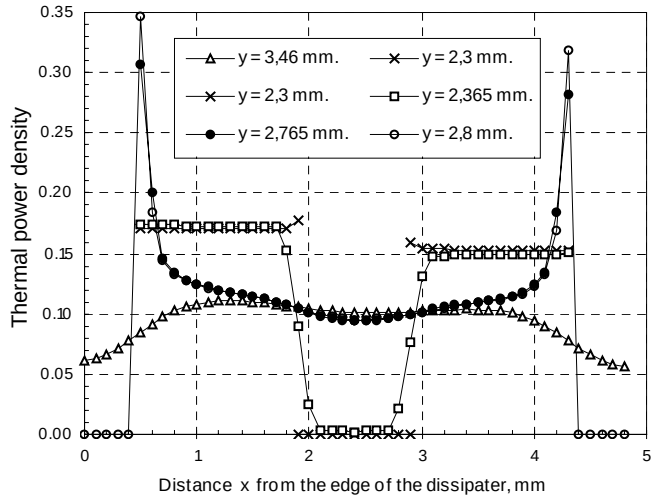

Figure 22. Total thermal power density (W/mm^2) in the hot side of the cell. T_c=273K, $\Delta T = 40^{\circ}\mathrm{C}$, I=4A.

The total thermal power distribution per unit area in the different surfaces between the thermoelements and the external surface of the hot outlet plate is shown in Fig. 22. The temperature of this plate remained constant owing to a boundary condition.

There is a damping of the thermal power peaks in the thermoelements as a consequence of the intermediate elements. The components located on top the thermoelements (electrical conductor (**ch**), soldering paste (**dh**) and plate (**eh**)) tends to uniform the thermal power distribution not only because they are good isotropic thermal conductors but the thermal power generated by Joule and Peltier effect is more uniform.

The same study was done in the cold face and the results were very similar.

As shown in Figs. 23 and 24. The relative differences between the thermal powers calculated with the numerical and analytical method showed in [1, chapter 5] are under 6% in the two cases ($\dot{Q}_c$, $\dot{Q}_h$).

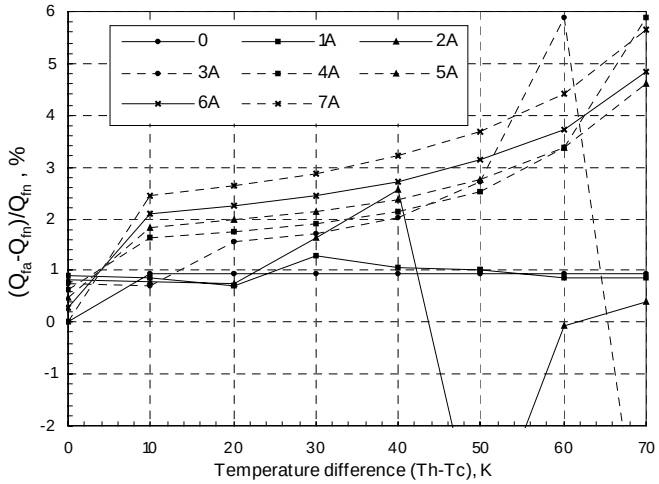

Figure 23. Relative differences in $\dot{Q}_c$ compared to the analytical model. Mode A, T_c=273K.

Working in the conditions of maximum efficiency or cop, the influence of the intermediate elements achieves relatives values from 4% to 16% for the cold face an lower values than 4% for the hot face (compared with the results of the elementary model).

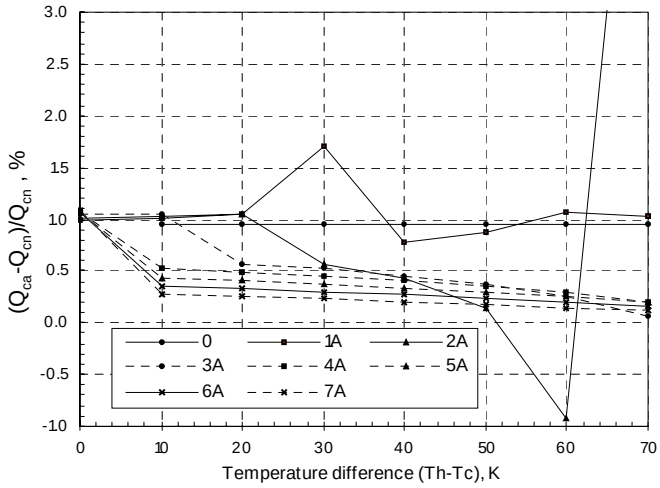

Figure 24. Relative differences in $\dot{Q}_h$ compared to the analytical model. Mode B, T_h=293K.

Temperature distribution.

This study was done with specific working conditions, $\Delta T = 40^{\circ}\mathrm{C}$, Tc=273K, I=4. The average temperature distributions in both thermoelements for the numeric, analytical and elementary model are shown in Fig. 25.

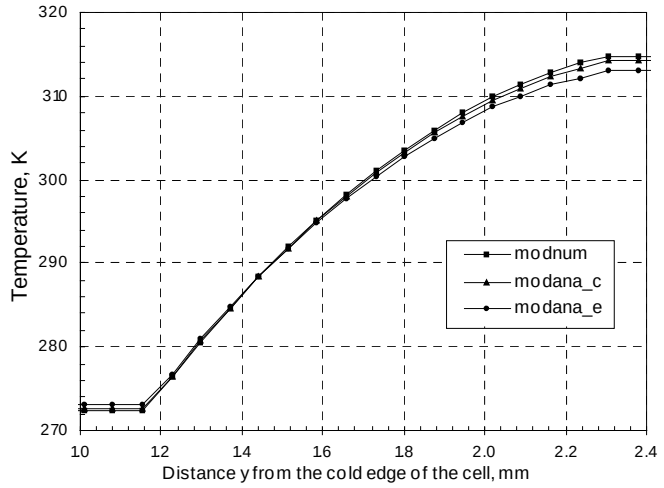

Figure 25. Average temperature distribution in the thermoelements, T_c=273K, $\Delta T = 40^{\circ}C$, I=4A.

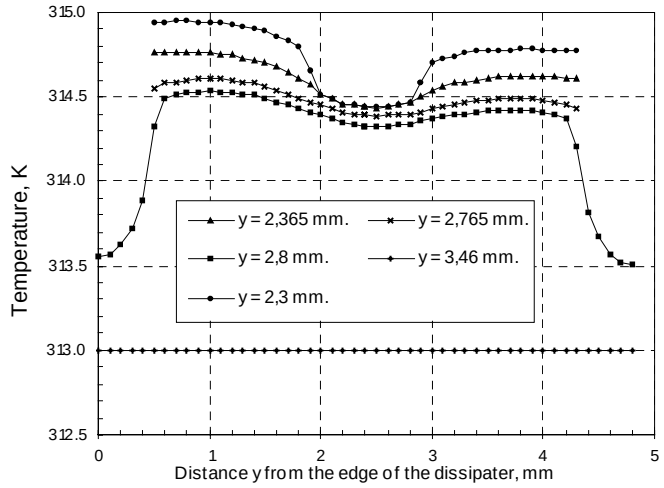

Figure 26. Temperature distribution in the unions between the intermediate elements at the hot side, T_c=273K, $\Delta T = 40^{\circ}C$, I=4A.

The results between the numeric and the analytical model were very similar. But the results found in the complex model were significantly different from the results in the elementary model. The temperature difference is 12.97% higher than in the elementary model. This discrepancy is attributed to the intermediate elements and it is more pronounced in the hot side. At last, the temperature distribution in the joins of the elements of the hot side is shown in Fig. 26. Taking into account that the temperature is constant in the external face of the heat exchanger, the flattening of the temperature distribution from the respective face of the themoelement is clear. It is also possible to observe the asymmetries in the influence area of each thermoelement owing to the asymmetry in the thermal powers generated by Peltier effect.

Conclusions

A study of a real thermoelectric cell using finite element techniques has been developed, considering that thermal and electrical flows were produced in two dimensions.

The methodology is based on the use of a commercial program which study Fourier and Joule effects in a coupled way, this program has been completed making a subroutine in order to incorporate the Peltier effect. Several models were analysed.

Firstly an elementary model, just considering thermoelectric elements, was studied. The great advantage of this analysis it that a mathematical solution exists and the numeric method can be validated. The errors were under 0.2% for $\dot{Q}_c$ and 0.02% for $\dot{Q}_h$, similar values were obtained for the efficiency and the *COP*. The differences between temperature distributions were smaller.

At last a complex model of a cell was analysed, in this case all the elements and materials of a commercial thermoelectric module are considered. The enormous possibilities of this tool have been stated. It is very easy to obtain numerical and graphical results of all the variables in all parts of the cell. The influence of the intermediate elements (welding, electrical bridges, dissipaters) can be evaluated contrasting the results between the complex and the elementary model.

Nomenclature

COP: Coefficient of performance, $\dot{Q}_h / \dot{W}_e$.

$\dot{Q}_c$: Amount of heat absorbed at cold face.

$\dot{Q}_h$: Amount of heat given away at hot face.

T_c : Temperature of the cold face during operation.

T_h : Temperature of the hot face during operation.

$\dot{W}_e$:Electrical power.

ε_f : Efficiency, $\dot{Q}_c / \dot{W}_e$

Anexxe 1

Elements	Material Fig. 7	Position Fig. 7	Dimensions (mm)		
			Height (y)	Width (x)	Length
Thermoelement (p)	**Bi2Te3**	**a1**	1.14	1.4	1
Thermoelement (n)	**Bi2Te3**	**a2**	1.14	1.4	1
Welding	**Sn-Bi**	**bf,bc**	0.065	1.9	1
Electric bridge	**Cu**	**cf,cc**	0.4	1.9	1
Welding	**Sn-Bi**	**df, dc**	0.035	1.9	1
Dissipaters	**Al2O3**	**ef,ec**	0.66	2..4	1

Properties of materials					
	Bi2Te3 (p)	**Bi2Te3 (n)**	**Al2O3**	**Sn**	**Cu**
λ W/(mK)	1.600	1.600	4.920E+01	6.000E+01	4.030E+02
ρ Ωm	9.000E-06	9.000E-06	1.000E+12	1.150E-07	1.440E-08
σ V/K	2.000E-04	-2.000E-04	3.000E-05	1.000E-05	1.400E-05
τ V/K	1.339E-04	-1.339E-04	-------	-------	-------

References

1. Arenas, A. Determinación de nuevos criterios que permitan la optimización de parámetros de diseño de una bomba de calor por efecto Peltier. (PhD Thesis. Universidad Pontificia Comillas. Madrid, 1999).
2. Palacios, R., Sanz-Bobi, M.A., *et al*, "Prototype of heat pump based on Peltier effect. Result of performance tests", *Proc. 2nd European Workshop on Thermoelectrics*, Nancy, France, November, 1995, pp. 93-97.